15TH IEA HEAT PUMP CONFERENCE
MAY 26–29, 2026 | HOFBURG
VIENNA 2026
DECARBONISATION THROUGH INNOVATION

Benchmarking and Validation of Reciprocating Piston Compressor Models for Industrial Heat Pump Design

Philip Widmaier[a], Leon Brendel[b], Dennis Roskosch[a], André Bardow[a], Emiliano Casati[a*]

[a]Energy and Process Systems Engineering, ETH Zurich, Tannenstrasse 3, 8092, Zurich, Switzerland
[b]Institute for Energy Systems, Eastern Switzerland University of Applied Sciences, Werdenbergstrasse 4, 9471, Buchs, Switzerland

Abstract

The economic viability of industrial heat pumps largely depends on compressor efficiency. Therefore, designing a heat pump requires selecting an appropriate compressor model. Several reciprocating compressor models have been introduced, each differing in approach and underlying physics. However, their relative strengths and weaknesses remain unclear. In this study, we examine three recently published compressor models: an empirical correlation, a loss-based model, and a differential model. We establish a comprehensive compressor performance dataset, by combining published experimental data and synthetic data generated with standardized compressor performance correlations (DIN EN 12900 + manufacturer coefficients). Over 20,000 data points are made publicly available with this work. We then use the dataset to evaluate the models' predictions across various refrigerants, operating points, and cylinder geometries relevant to industrial heat pumps. Our results show that both the correlation and the loss-based model deliver good prediction accuracy when properly fitted. These models predict compressor isentropic efficiency with average deviations of 2% to 6% across most of the investigated parameter space. Good accuracy is also demonstrated for out-of-sample refrigerants, including CO_2 and refrigerant mixtures. The loss-based model is more robust than the correlation for variations in compressor geometry. Both models are fast, with average runtimes on the order of milliseconds. The differential model, fitted to residential-regime compressor data but with greater physical detail, achieves lower accuracy and requires longer runtimes. Our findings suggest that targeted parameter re-fitting is more effective than adding physical detail for improving compressor efficiency predictions in industrial heat pump modeling.

Selection and/or peer-review under the responsibility of the organizers of the 15th IEA Heat Pump Conference 2026.

Keywords: Industrial high-temperature heat pumps, reciprocating compressor, model validation

1. Introduction

Electrifying process heat by industrial heat pumps (HPs) bears a substantial economic potential, offering more than one unit of heat per unit of electricity [1]. However, achieving good cycle efficiency requires sound system integration and often faces high capital costs. The economic viability of industrial HPs is strongly influenced by the compressor, affecting both operational costs through isentropic efficiency and capital costs through volumetric efficiency. Compressor efficiency, in turn, depends on the refrigerant, operating point, and compressor geometry. Thus, oversimplified compressor modeling (e.g., constant compressor efficiencies) can misguide the thermodynamic and economic assessment of HP processes [2]. For industrial HPs in the few-hundred-kilowatt capacity range, reciprocating compressors are the state-of-the-art technology [3].

Literature provides a wide variety of models for reciprocating compressors with varying levels of physical detail [3]. Yet, no benchmarking study compares different modeling approaches. Furthermore, reciprocating compressor models have not been validated for industrial HP applications. Most models are designed/fitted for low-temperature regimes (e.g., residential heating), and performance is mostly demonstrated for a narrow

* Corresponding author. Tel.: +41 44 632 47 94
E-mail address: casatie@ethz.ch

validation range [4–6]. Thus, the models' performance remains unclear across a wider or more diverse data range, introducing uncertainty into industrial HP design.

In this work, we benchmark and validate three recent reciprocating compressor models for industrial HP applications by introducing a comprehensive data set and evaluating their performance. The considered models are:

- **Doughty et al., 2024 [7]:** Empirical correlation, fitted to high-temperature experimental data of various pure refrigerants and their mixtures.
- **Roskosch et al., 2022 [8]:** Physically based loss estimation, fitted to experimental data of pure refrigerants at residential temperature ranges.
- **Neumaier et al., 2023 [9]**: Differential model with scaling rules for empirical valve flow correlations and fitting parameters.

The compressor models are described in more detail in Section 2.2. We evaluate compressor efficiency predictions over a range of refrigerants, operating points, and cylinder geometries relevant for industrial HPs. Validation data is generated from a compressor performance standard (DIN EN 12900 [10]) and coefficients published by manufacturers [11, 12]. The data generated for this work (Section 2.3) comprises over 20,000 data points and is provided in an open access repository [13].

2. Methods

2.1. Parameter ranges

A reciprocating compressor model for industrial HPs should perform reliably across relevant refrigerants, operating conditions, and compressor geometries. To validate predictions of the selected reciprocating compressor models (Section 2.2), we conduct a parameter study across the following industrially relevant parameter ranges:

- **Refrigerants**
  Most commercially available industrial HPs use hydrofluorocarbons (HFOs) as refrigerants [14]. Due to the phase-out of fluorinated refrigerants, industrial heat pumps increasingly use natural alternatives such as hydrocarbons.
- **Operating range**
  Industrial HP operating temperatures depend on the heat source (i.e., environmental or waste heat) and the heat sink (up to 200 °C), and are highly application-specific. Superheating at the compressor inlet can vary between 0 K and 35 K. [15]
  Compressor suction and discharge pressures depend on the refrigerant and can range from < 1 bar (low-temperature evaporation) to > 100 bar (e.g., transcritical CO_2 compression).
- **Compressor (cylinder) geometry**
  According to manufacturer portfolios [16, 17], reciprocating compressors for industrial heat pump applications typically feature 2 to 8 cylinders with diameters of 30 mm to 80 mm.

We assess compressor model performance considering ranges of suction and discharge temperatures/pressures. To obtain a differentiated assessment of model predictions, we vary one descriptive parameter at a time for each model input while keeping the others fixed, as detailed in Table 1.

Table 1: Fixed and varied (cf. gray-shaded table cells) model input parameters for model validation and benchmarking (Section 3.1). Each variation is conducted for a range of suction and discharge temperatures/pressures.
*: Temperature/pressure ranges under refrigerant variation are specific for each refrigerant considered.

Model		Model Input		Unit	Refrigerant variation (Figure 3)	Operating point variation (Figure 4)	Geometry variation (Figure 4)
Correlation [7]	Loss-based model [8] and differential model [9]	Refrigerant	Refrigerant (properties)	−	Propane, R1234ze(E), CO2	R1234ze(E)	R1234ze(E)
Correlation [7]	Loss-based model [8] and differential model [9]	Operating point	Evap. temperature Suction pressure	°C bar	−25 … 20* 2.4 … 39*	0 … 20	0 … 20
Correlation [7]	Loss-based model [8] and differential model [9]	Operating point	Cond. temperature Discharge pressure	°C bar	20 … 90* 8.3 … 105*	60 … 95	60 … 95
Correlation [7]	Loss-based model [8] and differential model [9]	Operating point	Superheating	K	15	10,20,30	15
	Loss-based model [8] and differential model [9]	Geometry	Bore	mm	50	50	30,50,65
	Loss-based model [8] and differential model [9]	Geometry	Stroke	mm	31, 39.3	39.3	39.3
	Loss-based model [8] and differential model [9]	Geometry	# of cylinders	−	4	4	2, 4
	Loss-based model [8] and differential model [9]	Geometry	Elec. frequency	Hz	50	50	50

2.2. Compressor models

Reciprocating compressor models vary in their level of physical detail: Models with a lower level of physical detail are mostly correlations between experimental data and compressor efficiency that do not give any physical information about processes inside the compressor. Modeling at a higher level of physical detail usually involves numerical methods to solve the differential equations from conservation laws, capturing the most important physical compressor processes. [18]

Although adding physical detail can improve model predictions beyond the experimental data range (out-of-sample), it typically requires iterative solutions of nonlinear equations (e.g., energy and mass balances), increasing computational cost. In this study, we compare three recent reciprocating piston compressor models:

The correlation by Doughty et al. (2024) [7] describes the overall isentropic and volumetric efficiency in single-line equations containing only a few terms. The empirical equations were formulated to ensure physical plausibility. The correlation accounts for suction state and discharge pressure but does not explicitly include compressor geometry. It uses nine fitting parameters, including one refrigerant-dependent toggle that distinguishes hydrocarbons from HFOs. The correlation is fitted to experimental high-temperature HP data for pure refrigerants and their mixtures [19]. In this study, we use the correlation as published. With an average runtime[1] of 0.9 ms, it is the fastest model in the study.

The loss-based model by Roskosch et al. (2022) [8] predicts compressor efficiency through a physically based loss estimation method (detailed equations provided in the Appendix). It accounts for refrigerant properties such as specific heat capacity and molar mass, as well as suction state and discharge pressure. The model explicitly incorporates cylinder geometry into its formulation and employs five fitting parameters, two of which are scaled relative to the (reference) fitting compressor based on the cylinder geometry. The loss-based model was originally fitted to small-scale compressor data at residential operating conditions and is refitted here for an industrial context (Section 2.4). The average runtime[1] is 3.2 ms.

The differential model by Neumaier et al. (2023) [9] is an implementation of work by Roskosch et al. [20] in Rust [21]. Based on a standard differential modeling approach for reciprocating compressors [4], the model features two empirical correlations for valve flows to capture refrigerant-dependent physics, and uses two fitting parameters for friction pressure and the height of the clearance volume. Neumaier et al. add scaling rules based on cylinder bore and stroke to transfer correlations and model parameters to other compressor geometries. The differential model was fitted to 25 experimental data points for five different refrigerants at

[1] The model runtimes were determined on a system equipped with an AMD Ryzen 7 PRO 8840U processor (3.30 GHz), 32 GB of RAM, and Radeon 780M graphics.

residential operating conditions [20]. In this work, we use the model as published, operating at an average runtime[1] below 5 s.

The correlation and the loss-based model are implemented using fluid property data from REFPROP [22]. The differential model relies on the PC-SAFT equation of state [23] with parameters from Esper [24] and Poling [25] implemented in the FeOs framework for thermodynamic equations of state [26].

2.3. Reference data

We generate reference data using DIN EN 12900 polynomials [10] with coefficients provided by compressor manufacturers [11, 12]. The ten-coefficient polynomials represent standardized empirical correlations for compressor performance data. DIN EN 12900 coefficients are subject to validity ranges that depend on evaporation and condensation temperature or suction and discharge pressure (depending on subcritical/transcritical compression and the polynomial fit). Within a given validity range, coefficients are specific to the refrigerants, operating point (i.e., superheating), and compressor geometry.

We use the following validation data generation procedure for each compressor geometry and superheating:

- Query of DIN EN 12900 coefficients for the refrigerant mass flow $\dot{m}$ and electrical power consumption P_{elec} from the manufacturer database
- Calculation of mass flow and electrical power consumption using DIN EN 12900 polynomials
- Determination of the enthalpy difference for isentropic compression Δh_{is} to calculate the isentropic compression power P_{is} (fluid property data from REFPROP)
- Calculation of the overall isentropic efficiency:

$$\eta_{\mathrm{is,o}} = \frac{P_{\mathrm{is}}}{P_{\mathrm{elec}}} = \frac{\dot{m}\Delta h_{\mathrm{is}}}{P_{\mathrm{elec}}} \tag{1}$$

The tolerance for quantities determined using the DIN EN 12900 polynomials is certified to be <5% [27]. A comprehensive database comprising compressor efficiencies for more than 20,000 reference data points of various refrigerants (hydrocarbons, HFOs, CO_2), operating points, and geometries is published with this work.

2.4. Re-fitting of the loss-based compressor model

The loss-based compressor model by Roskosch et al. [8] was originally designed/fitted for predicting compressor efficiency in residential heating applications. For benchmarking against the correlation (fitted to high-temperature HP data) and the differential model, we re-fit the loss-based model to data at industrial parameter ranges (Section 2.1).

Re-fitting employs only pure refrigerant (not mixture) data, since tests showed that including mixture data during fitting impairs in-sample prediction accuracy. However, satisfactory prediction of mixture compressor efficiency can be achieved if the mixture's components are well-predicted (cf. Section 3.2).

Base of the fitting data is an experimental dataset from a lab-scale HP setup and features a selection of industry-relevant hydrofluoroolefins (HFOs) + butane (red area, Figure 1, bottom right plot) [19]. The experimental dataset covers industrial temperature ranges (red dots, Figure 1, left plot) and employs two (similar) cylinder geometries with a bore of 50 mm and a stroke of 39.3 mm and 40 mm, respectively (red circles, Figure 1, top right plot). Even though high temperature ranges are well-represented, the experimental dataset is not diverse in substance groups and cylinder geometry, and hence does not cover the required parameter range (Section 2.1).

Thus, the experimental dataset is expanded with DIN EN 12900 reference data (Section 2.3, compare blue elements in Figure 1). Data points for propane and propene are added at the highest possible temperature ranges (limited by DIN EN 12900 coefficient validity). The hydrocarbon data is spread over diverse cylinder geometries (bore 30 – 65 mm, stroke 33 – 42 mm). The experimental compressor's cylinder geometry (50 mm bore and 39.3 mm stroke) was chosen as parameter scaling reference during fitting, as it corresponds to most data points in the fitting dataset and represents a mid-range cylinder size.

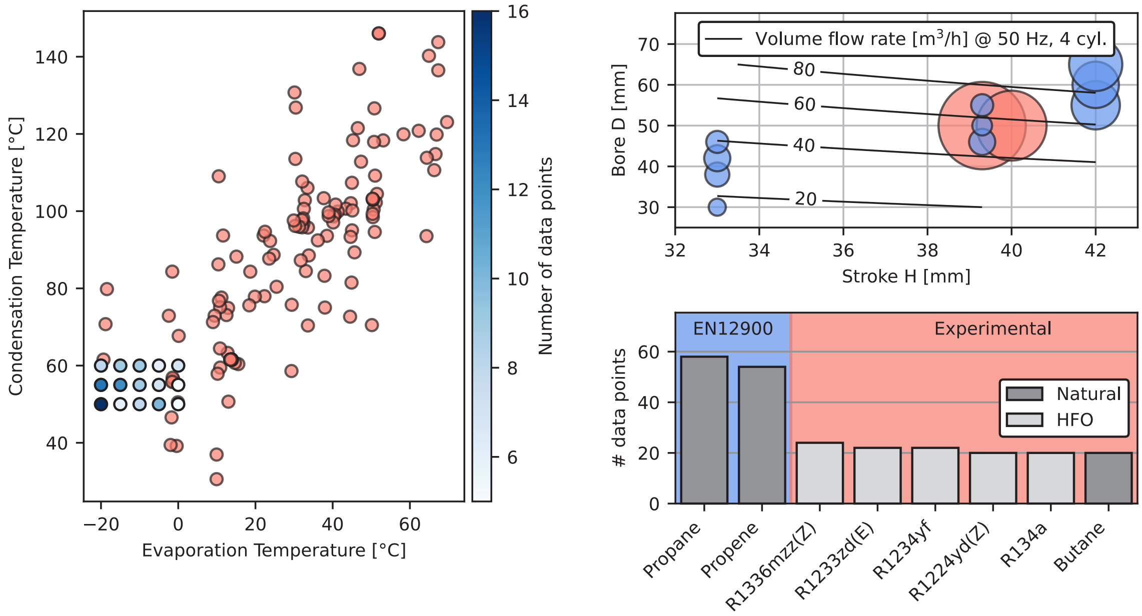

Figure 1: Fitting data overview. Red highlights experimental data, blue highlights reference data generated with DIN EN 12900 polynomials and manufacturer coefficients.
Top right plot: The size of circles represents the number of corresponding data points.

To quantify the model prediction accuracy for the different fits, we use the Mean Absolute Relative Difference (MARD) relative to the experimental dataset. The MARD of the overall isentropic efficiency is expressed as a percentage of the experimental values, where N represents the number of experimental data points, $\eta_{\mathrm{is,o}}^{\mathrm{exp,i}}$ denotes the experimental (measured) value, and $\eta_{\mathrm{is,o}}^{\mathrm{pred,i}}$ represents the predicted value for the i-th data point.

$$\mathrm{MARD} = \frac{1}{\mathrm{N}} \sum_{\mathrm{i=1}}^{\mathrm{N}} \frac{\left| \eta_{\mathrm{is,o}}^{\mathrm{pred,i}} - \eta_{\mathrm{is,o}}^{\mathrm{exp,i}} \right|}{\eta_{\mathrm{is,o}}^{\mathrm{exp,i}}} \cdot 100\% \tag{2}$$

As the loss-based model was initially fitted to data of residential heat pumps, predicting the (high-temperature) experimental dataset results in significant prediction errors (Figure 2, "as published"). Re-fitting the loss-based model using the experimental dataset reduces the MARDs to around 4 % (in-sample; Figure 2, "experimental dataset") indicating reliable reproduction of high-temperature data. Expanding the experimental dataset with DIN EN 12900 data retains low MARDs for predicting the experimental dataset (Figure 2, "expanded dataset") and promises better general prediction performance and reliable parameter scaling.

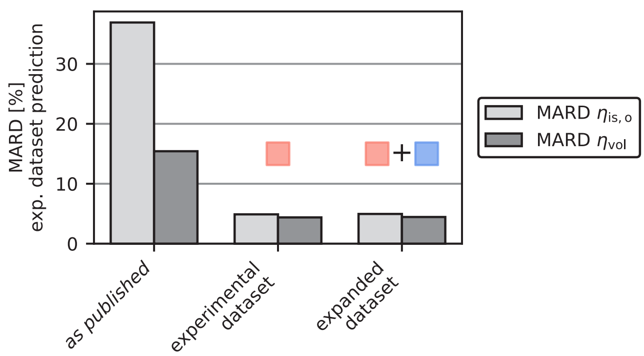

Figure 2: MARD of loss-based model efficiency predictions for the experimental dataset (red plot elements in Figure 1), expressed as a percentage of the experimental efficiencies.
The model as published is compared to refits on the experimental and expanded dataset (red + blue plot elements in Figure 1) .

We hence use the model parameters re-fitted to the expanded dataset (Table 2, “Re-fitted value”), as defined by the loss-based model’s governing equations (cf. Appendix). Compared to the original fit (Table 2, “Value as published”), the model parameters for friction losses a and flow losses b increased substantially, which can be explained by the larger cylinder geometries in the expanded dataset. Because the scaling rules were active during re-fitting, the parameters were adjusted accordingly. The electrical loss coefficient c more than quadrupled, suggesting it may account for additional constant losses that increase in larger machines (e.g., increased crankshaft/bearing friction due to a larger number of cylinders). At the same time, the significant value highlights the model’s flexibility: physical effects do not necessarily map cleanly onto the parameters meant to represent them. The model parameter associated with the compressor clearance volume k_1 decreased, following the trend toward higher volumetric efficiency for larger cylinders. Finally, the overcompression factor k_2 increased, which can be explained by the large pressure ratios represented in the expanded dataset.

Table 2: Loss-based model fitting parameters.

Parameter affiliation	Friction loss	Flow loss	Electrical loss	Clearance volume	Overcompression
Unit	W	m^{-4}	–	mm	$\mathrm{m}^2/\mathrm{s}^2$
Fitting parameter	a	b	c	k_1	k_2
Value as published (Roskosch et al. [8])	91.59	$12.11 \cdot 10^6$	0.062	3.49	$7.19 \cdot 10^3$
Re-fitted value (this work)	189.54	$39.96 \cdot 10^6$	0.277	2.33	$10.93 \cdot 10^3$

3. Results

3.1. Model validation and benchmarking

The presented results focus on the overall isentropic compressor efficiency, which is decisive for determining HP cycle efficiency. For validation and benchmarking, we vary the model input parameters across industrial ranges (Section 2.1, cf. Table 1) and compare against reference data generated with DIN EN 12900 polynomials and manufacturer coefficients (Section 2.3).

Refrigerant variation

We first assess efficiency prediction accuracy under variation of the refrigerant (Figure 3) while other model inputs are kept constant. Operating temperatures/pressures are set as high as the validation data allows for each refrigerant.

We chose three refrigerants from different substance groups with high relevance for industrial applications [14, 15] and abundant DIN EN 12900 coefficients [11, 12]. The hydrocarbon Propane, one of the most common natural refrigerants, is included in the fitting dataset for the correlation- and loss-based model and was used to fit the semi-physical correlations and fitting parameters of the differential model. R1234ze(E) is widely regarded as a substitute for conventional HFOs [14] and offers high-temperature DIN EN 12900 validity ranges. R1234ze(E) is not contained in any of the models’ fitting datasets; however, other HFOs are well represented. CO_2 (natural) is highly relevant in heating/cooling due to its beneficial properties (e.g., non-flammable, non-toxic). CO_2 stands out because it is neither a hydrocarbon nor an HFO; no similar refrigerants are included in the fitting datasets of any model. Its high pressure levels and specific cylinder designs make it well-suited for testing how the compressor models handle out-of-sample prediction.

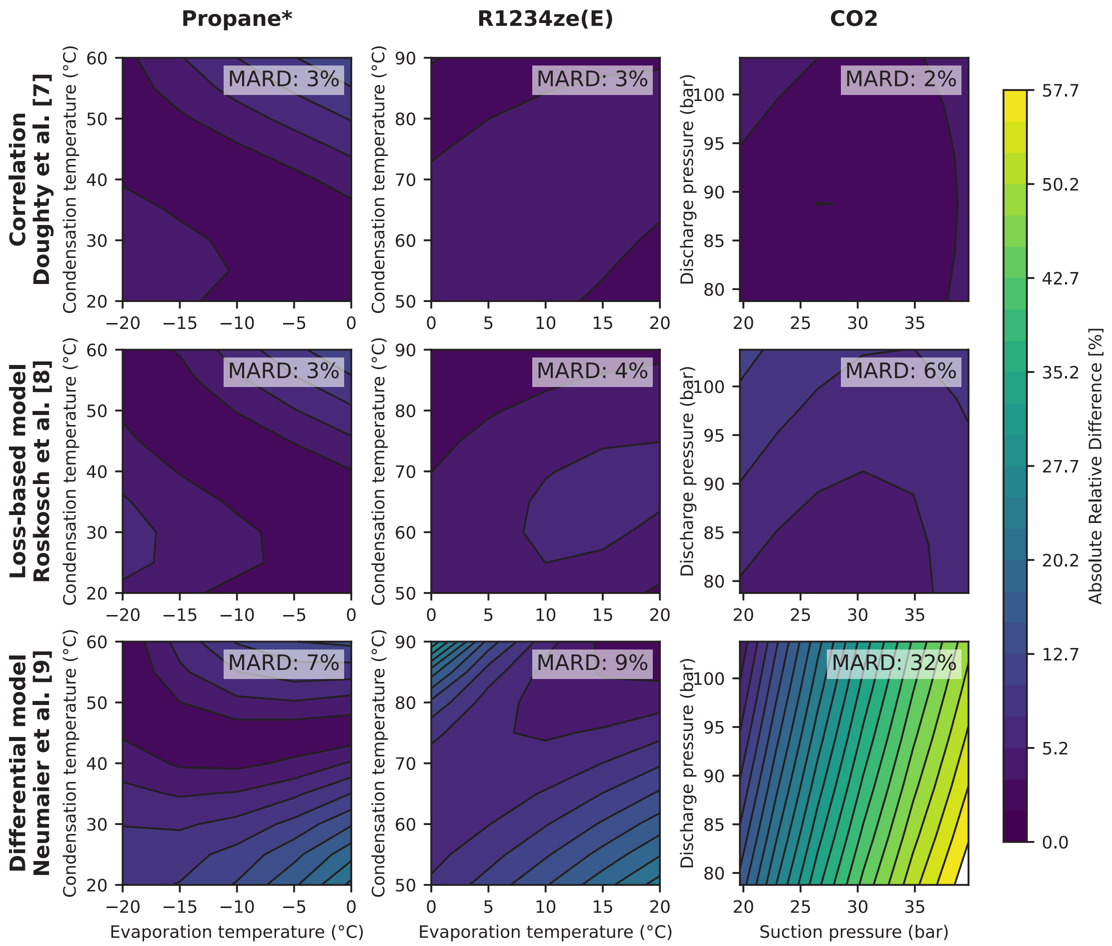

Figure 3: Absolute Relative Difference between overall isentropic efficiency predictions from the considered models and validation data for refrigerants propane, R1234ze(E) and CO_2. For subcritical compression (Propane and R1234ze(E)), evaporation and condensation temperatures are varied. For transcritical compression (CO_2), suction and discharge pressures are varied.
All remaining model input parameters are fixed (Table 1).
*Propane is included in the fitting data of each model

Among the models, the correlation yields the lowest MARDs (2 ... 3%), followed by the loss-based model (3 ... 6%). Neither model shows deviation hotspots over the considered range of evaporation and condensation temperatures (pressures), nor any significant refrigerant or in-/out-of-sample bias.

The differential model exhibits MARDs of 7% and 9% for propane and R1234ze(E), respectively. A slight increase in deviation is observed at high suction and/or condensation temperatures. For CO_2, significant deviations (up to 56%) from the differential model's predictions are observed, increasing with suction pressure and resulting in a large MARD of 32% over the full operating range. The deviations are attributed to the empirical correlations for the effective valve flow areas in the differential model, which are fitted to hydrocarbon and HFO data. The high mass fluxes of CO_2 lead to an underestimation of the discharge valve flow areas and, consequently, to an underestimation of the compressor's overall isentropic efficiency. We choose R1234ze(E) as the refrigerant for further parameter variation, as all models show low MARDs for R1234ze(E), indicating no refrigerant-specific bias. Moreover, DIN EN 12900 coefficients for R1234ze(E) are available at high-temperature validity ranges.

Operating point & geometry variation

The following results are shown exclusively as MARD values, since no notable variations occur over the range of evaporation and condensation temperatures (Figure 4).

The superheating remains as the determining variable for the operating point and is varied (10,20,30 K) while the evaporation/condensation temperature ranges and other model inputs are fixed (Table 1). Superheating variation results in nearly constant MARDs in line with the ones during refrigerant variation, indicating that varied superheating does not trigger notable deviations in prediction quality for any model (Figure 4, left).

To assess efficiency prediction accuracy under variation of the cylinder geometry, the cylinder bore is chosen as a variable geometry input, while all other model inputs are kept constant. The bore indicates the cylinder volume, since the ratio of bore and stroke usually lies within a narrow range close to 1 [8].

Generally, variation of the cylinder bore results in efficiency prediction MARDs in line with values for the refrigerant and superheating variation (Figure 4). However, all models show increased deviations for the smallest bore of 30 mm. The correlation does not explicitly account for cylinder geometry for efficiency prediction. Effects of the geometry on compressor efficiency are instead lumped into the correlation's nine fitting parameters. Since the correlation was fitted to experimental data from 50 mm bore compressors, inaccuracies for different geometries are to be expected. The loss-based model uses bore- and stroke-dependent scaling rules to transfer model parameters across cylinder geometries. The scaling rules were active during model re-fitting to a geometry-variable dataset (Section 2.4). The fitting parameters' values are hence consistent with the scaling rules, keeping deviations for other cylinder geometries moderate. The differential model employs scaling rules as well; However, the model was fitted to data from a single 34 mm bore compressor, meaning the fitting parameter values are not aligned with the scaling rules (inactive during fitting). As a result, the non-linear scaling rules can lead to overestimation of parameter values during downscaling to smaller cylinders, resulting in underestimated isentropic efficiency and increased MARD.

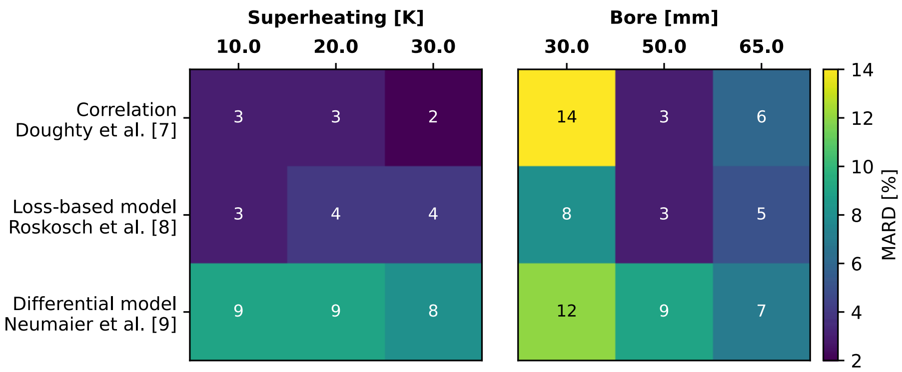

Figure 4: Mean Absolute Relative Deviations (MARDs) between compressor model overall isentropic efficiency predictions and validation data for varying superheating (left) and varying cylinder bore (right). All remaining model input parameters are fixed (Table 1).

3.2. Refrigerant Mixtures

Finally, the capability to predict mixture efficiency is examined. Only results for the correlation and the loss-based model are shown, as the differential model is currently not implemented for mixture property data.

Model efficiency predictions are compared to experimental data for one HFO mixture, R1233ze(E)/R1234yf, and one hydrocarbon mixture, butane/propane (Figure 5). The experimental mixture data are part of the correlation's fitting dataset (in-sample prediction), whereas the loss-based model was fitted only to data of the pure mixture components.

Both models show acceptable prediction accuracies, with the loss-based model demonstrating good prediction of mixture efficiencies despite being fitted solely to pure refrigerant data. Composition-dependent

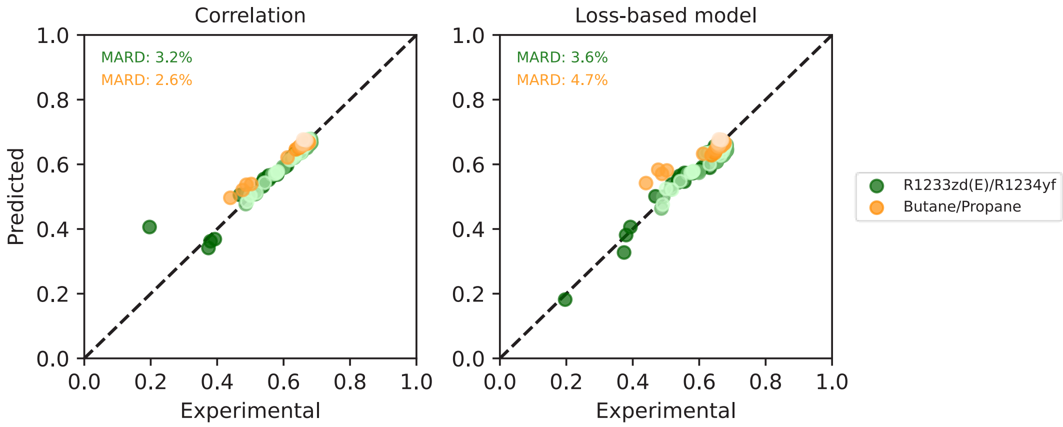

Figure 5: Mixture overall isentropic efficiency predictions versus experimental results.
Darkness of color represents the molar share of the first mixture component:
R1233zd(E)/R1234yf: 0.52 ... 0.83; butane/propane: 0.1 ... 0.58
The correlation's fitting dataset contains the mixture data shown, the loss-based model was fitted to the pure components' data only.

differences in accuracy are not observed. No notable substance-group-dependent differences in mixture prediction accuracy are observed, with similar MARDs for the HFO and hydrocarbon mixtures in each model. The correlation, since it was fitted exclusively to high-temperature data, shows some deviation at low suction pressure (cf. outlier in Figure 5, left).

4. Conclusion

This study compared the accuracy of different compressor models to predict efficiency in an industrial heat pump (HP) modeling context. Three reciprocating compressor models – a correlation, a loss-based model, and a differential model – were considered. While employing increasing levels of physical detail, all models rely on correlations and parameters fitted to experimental data. In the study, the compressor models were evaluated for industrially relevant refrigerants, operating points, and geometries. Reference data was generated from DIN EN 12900 polynomials using manufacturer-published coefficients. Input parameter variations were conducted across a range of suction and discharge conditions. The prediction error was quantified using the Mean Absolute Relative Deviation (MARD, expressed as a percentage of the experimental efficiencies) of the overall isentropic compressor efficiency.

Varying the refrigerant revealed the lowest MARDs for the correlation and loss-based model (2 ... 6%), with no notable bias across substance groups or between in-/out-of-sample data. The differential model showed larger deviations (7 ... 9%) with a strong increase for CO_2 (32%, out-of-sample refrigerant). Varying the operating point (i.e., superheating at fixed suction and discharge pressure) showed low deviations for all models (correlation $\approx 3\%$ to the differential model $\approx 9\%$). Varying cylinder geometries (i.e., cylinder bore) were well predicted for cylinders larger than or equal to those represented in the fitting data. Predictions of smaller cylinder geometries increased MARDs across all models, with the loss-based model achieving the smallest deviations at 8%.

Across the three models examined, the study found no clear relationship between the level of physical modeling detail and prediction accuracy. However, the correlation's increased prediction error during geometry variation demonstrates that modeling should not only account for the influence of refrigerants and operating points, but also geometry to provide reliable efficiency predictions.

Further, targeted re-fitting significantly improved the loss-based model's prediction accuracy, highlighting the necessity of an appropriate fitting dataset to achieve accurate and reliable efficiency predictions. The differential model's accuracy could thus be improved by refitting its semi-physical correlations and parameters to high-temperature data.

Finally, runtimes tend to increase with higher levels of physical modeling detail (e.g., between the correlation and the differential model). For industrial HP modeling, compressor model performance (accuracy and runtime) would likely benefit more from appropriate fitting than from increased physical detail, provided sufficient data is available.

Nomenclature

Symbol	Unit	Description
a	W	Friction loss coefficient
b	$\mathrm{m^{-4}}$	Flow loss coefficient
c	—	Electrical loss coefficient
c_p	$\mathrm{J \cdot kg^{-1} \cdot K^{-1}}$	Specific isobaric heat capacity
c_v	$\mathrm{J \cdot kg^{-1} \cdot K^{-1}}$	Specific isochoric heat capacity
f_mech	Hz	Mechanical frequency
Δh_is	$\mathrm{J \cdot kg^{-1}}$	Specific enthalpy at isentropic compression
k_1	mm	Clearance volume loss coefficient
k_2	$\mathrm{m^2 \cdot s^{-2}}$	Over-compression loss coefficient
$\dot{m}$	$\mathrm{kg \cdot s^{-1}}$	Mass flow rate
n_cyl	—	Number of cylinders
p	Pa	Pressure
P_elec	W	Electrical power input
P_is	W	Isentropic power
V_cyl	$\mathrm{m^3}$	Cylinder volume
$\eta_\mathrm{is,o}$	—	Overall isentropic efficiency
η_vol	—	Volumetric efficiency
ρ	$\mathrm{kg \cdot m^{-3}}$	Density

Index		
dis		Discharge state at compressor outlet
exp		Experimental value
pred		Predicted value
suc		Suction state at compressor inlet

Acknowledgements

We thank Bitzer Kühlmaschinenbau GmbH and Danfoss for providing access to their DIN EN 12900 coefficients used in this publication. This work was funded by BRIDGE as part of the project "High-Efficiency High-Temperature Heat Pumps with Temperature Glide". We are grateful to the Swiss National Science Foundation SNSF and Innosuisse for their support.

Compressor performance data

The reference dataset generated in the course of this work can be accessed under: https://doi.org/10.5281/zenodo.17599603 [13]

Conflict of interest

The authors declare the following financial interests and personal relationships that could be considered as potential competing interests: André Bardow has served on review committees for research and development at ExxonMobil and TotalEnergies. André Bardow holds ownership interests in firms that provide services to industry, some of which may be related to industrial heating. The remaining authors declare no known competing financial interests or personal relationships that could have influenced the work reported in this paper.

Appendix: Governing equations of the loss-based model

The loss-based model by Roskosch et al. [8] takes into account the isentropic compression power P_{is} and cumulative compressor losses P_{loss} to determine the overall isentropic compressor efficiency $\eta_{\mathrm{is,o}}$. Modeling focuses on first-order loss effects and maintains a semi-physical approach. Each loss power is affiliated with a fitting parameter (friction losses: a, flow losses: b, and electrical losses: c).

$$\eta_{\mathrm{is,o}} = \frac{P_{\mathrm{is}}}{P_{\mathrm{is}} + P_{\mathrm{loss}}} = \frac{P_{\mathrm{is}}}{\left(P_{\mathrm{is}} + a + b\,\frac{\dot{m}^3}{\rho_{\mathrm{suc}}^2}\right) \cdot \frac{1}{1-c}} \tag{A1}$$

Both the isentropic compression power P_{is} and the flow losses depend on the mass flow rate $\dot{m}$, which is determined by the volumetric compressor efficiency η_{vol}.

$$\dot{m} = V_{\mathrm{cyl}} \cdot n_{\mathrm{cyl}} \cdot f_{\mathrm{mech}} \cdot \rho_{\mathrm{suc}} \cdot \eta_{\mathrm{vol}} \tag{A2}$$

The volumetric compressor efficiency η_{vol} is modelled based on isentropic re-expansion of the gas in the clearance volume. Since the exact height of the clearance volume is typically unknown for a specific reciprocating piston compressor, it is represented by a fitting parameter k_1. The fitting parameter k_2 covers effects of overcompression and non-ideal deviations from isentropic re-expansion.

$$\eta_{\mathrm{vol}} = 1 - \frac{k_1}{H}\left(\left(\frac{p_{\mathrm{dis}} + k_2 \cdot p_{\mathrm{suc}}}{p_{\mathrm{suc}}}\right)^{c_{\mathrm{v}}/c_{\mathrm{p}}} - 1\right) \tag{A3}$$

References

[1] G. P. Thiel and A. K. Stark, "To decarbonize industry, we must decarbonize heat," *Joule*, vol. 5, no. 3, pp. 531–550, 2021, doi: 10.1016/j.joule.2020.12.007.

[2] D. Roskosch, V. Venzik, J. Schilling, A. Bardow, and B. Atakan, "Beyond Temperature Glide: The Compressor is Key to Realizing Benefits of Zeotropic Mixtures in Heat Pumps," *Energy Tech*, vol. 9, no. 4, p. 2000955, 2021, doi: 10.1002/ente.202000955.

[3] T. El Samad, A. Żabnieńska-Góra, H. Jouhara, and A. I. Sayma, "A review of compressors for high temperature heat pumps," *Thermal Science and Engineering Progress*, vol. 51, p. 102603, 2024, doi: 10.1016/j.tsep.2024.102603.

[4] T. Dutra and C. J. Deschamps, "A simulation approach for hermetic reciprocating compressors including electrical motor modeling," *International Journal of Refrigeration*, vol. 59, pp. 168–181, 2015, doi: 10.1016/j.ijrefrig.2015.07.023.

[5] M. Farzaneh-Gord, A. Niazmand, M. Deymi-Dashtebayaz, and H. R. Rahbari, "Thermodynamic analysis of natural gas reciprocating compressors based on real and ideal gas models," *International Journal of Refrigeration*, vol. 56, pp. 186–197, 2015, doi: 10.1016/j.ijrefrig.2014.11.008.

[6] G. Z. Santos, A. F. Ronzoni, and C. J. Hermes, "Performance characterization of small variable-capacity reciprocating compressors using a minimal dataset," *International Journal of Refrigeration*, vol. 107, pp. 191–201, 2019, doi: 10.1016/j.ijrefrig.2019.07.014.

[7] O. Doughty, C. Arpagaus, S. S. Bertsch, and L. P. M. Brendel, "Set of Performance Correlations for Reciprocating Compressor Covering Synthetic and Hydrocarbon Refrigerants," 2024.

[8] D. Roskosch, C. Arpagaus, S. Bertsch, and A. Bardow, "Compressor Design Vs. Refrigerants Properties: What Affects Compressor Efficiency More?," *International Compressor Engineering Conference*, 2022.

[9] L. Neumaier, D. Roskosch, J. Schilling, G. Bauer, J. Gross, and A. Bardow, "Refrigerant Selection for Heat Pumps: The Compressor Makes the Difference," *Energy Tech*, p. 2201403, 2023, doi: 10.1002/ente.202201403.

[10] DIN-Normenausschuss Kältetechnik (FNKä), "DIN EN 12900, Kältemittel-Verdichter – Nennbedingungen, Toleranzen und Darstellung von Leistungsdaten; Deutsche und Englische Fassung prEN 12900:2023," 2024.

[11] Bitzer Kühlmaschinenbau GmbH, *BITZER Software*: Bitzer Kühlmaschinenbau GmbH, 2025. [Online].

Available: https://www.bitzer.de/websoftware/
[12] Bock GmbH, *BOCK VAP*: Danfoss Climate Solutions, 2025. [Online]. Available: https://vap.bock.de/
[13] P. Widmaier, L. P. M. Brendel, D. Roskosch, A. Bardow, and E. Casati, *Compressor Performance Data.* [Online]. Available: https://doi.org/10.5281/zenodo.17599603
[14] J. Sun, P. Wang, L. Gao, K. Nawaz, and E. Vineyard, "A Comprehensive Review of Working Fluids for High-Temperature Heat Pumps: History, Selection, and Evaluation," *Journal of Thermal Science and Engineering Applications*, pp. 1–42, 2025, doi: 10.1115/1.4070129.
[15] C. Arpagaus, F. Bless, M. Uhlmann, J. Schiffmann, and S. S. Bertsch, "High temperature heat pumps: Market overview, state of the art, research status, refrigerants, and application potentials," *Energy*, vol. 152, pp. 985–1010, 2018, doi: 10.1016/j.energy.2018.03.166.
[16] Bitzer Kühlmaschinenbau GmbH, "ECOLINE: semi-hermetic single-stage reciprocating compressors for standard refrigerants," 2025.
[17] Danfoss A/S, "HG, HA, HGZ semi-hermetic compressors," *BOCK VAP*, 2025. [Online]. Available: https://assets.danfoss.com/documents/320034/AD464059718960en-000101.pdf
[18] E. Navarro, E. Granryd, J. F. Urchueguía, and J. M. Corberán, "A phenomenological model for analyzing reciprocating compressors," *International Journal of Refrigeration*, vol. 30, no. 7, pp. 1254–1265, 2007, doi: 10.1016/j.ijrefrig.2007.02.006.
[19] L. P. Brendel, S. N. Bernal, N. Lüchinger, C. Arpagaus, and S. S. Bertsch, "Experimental data of a reciprocating compressor across wide range of refrigerants and operating conditions," *International Journal of Refrigeration*, vol. 182, pp. 409–417, 2026, doi: 10.1016/j.ijrefrig.2025.11.012.
[20] D. Roskosch, V. Venzik, and B. Atakan, "Thermodynamic model for reciprocating compressors with the focus on fluid dependent efficiencies," *International Journal of Refrigeration*, vol. 84, pp. 104–116, 2017, doi: 10.1016/j.ijrefrig.2017.08.011.
[21] The Rust Team, "The Rust programming language (Version 1.91.0)," 2024. [Online]. Available: https://www.rust-lang.org/
[22] Lemmon, E.W., Bell, I.H., Huber, M.L., McLinden, M.O., *REFPROP: Reference Fluid Thermodynamic and Transport Properties*. Standard Reference Data Program. Gaithersburg: National Institute of Standards and Technology NIST, 2018.
[23] J. Gross and G. Sadowski, "Perturbed-Chain SAFT: An Equation of State Based on a Perturbation Theory for Chain Molecules," *Ind. Eng. Chem. Res.*, vol. 40, no. 4, pp. 1244–1260, 2001, doi: 10.1021/ie0003887.
[24] T. Esper, G. Bauer, P. Rehner, and J. Gross, "PCP-SAFT Parameters of Pure Substances Using Large Experimental Databases," *Ind. Eng. Chem. Res.*, vol. 62, no. 37, pp. 15300–15310, 2023, doi: 10.1021/acs.iecr.3c02255.
[25] B. E. Poling, J. M. Prausnitz, and J. P. O'Connell, *The properties of gases and liquids,* 5th ed. New York: McGraw-Hill, 2001.
[26] P. Rehner, G. Bauer, and J. Gross, "FeO s : An Open-Source Framework for Equations of State and Classical Density Functional Theory," *Ind. Eng. Chem. Res.*, vol. 62, no. 12, pp. 5347–5357, 2023, doi: 10.1021/acs.iecr.2c04561.
[27] Air-Conditioning, Heating, and Refrigeration Institute, "Tolerances and Uncertainties in Performance Data of Refrigerant Compressors," *ASERCOM Guidelines*, 2017.